

Chapter 32

Complex universality

In its original form, the existence of δ seems a technical analytic result. Now it proves to be an aspect of a broader property of fractal scaling.

—Benoit B. Mandelbrot

THE EASY PART of dynamical systems theory is the regular, “ordered” motions; attracting fixed points and limit cycles, integrable “elliptic” regions. As we now know, fully chaotic dynamics is often not much harder: it can be described by Smale horseshoes, finite grammars and unstable periodic orbits. The hard part lies in between, the dynamics to which we shall refer to here as the “border of order” - trajectories that are neither stable nor unstable.

The closer to the border of order, the harder it is to decide whether a given trajectory is stable or unstable. We need to inspect the trajectory with a higher and higher resolution, for longer and longer times, as in figure 32.1. In general this is a hopeless undertaking. However, there are situations where the border of order is a self-similar fractal. By a magnification of spatial scales and a replacement of time by logarithmic time, the dynamics close to the border of order can be turned into a clean, uniformly hyperbolic dynamics, and described to exponential accuracy by techniques developed for nice chaotic sets. Not only that, but the fine structure of the border turns out to be topologically and quantitatively universal, i.e., common to large classes of dynamical systems.

In this chapter we illustrate the key concepts underlying the renormalization theory of transitions to chaos by studying sequences of period n -tuplings for complex maps. We have chosen this example for its beauty and simplicity; here you should be able to visualize the renormalization transformations and the universal scalings as encodings of the self-similar patterns generated by deterministic dynamics.

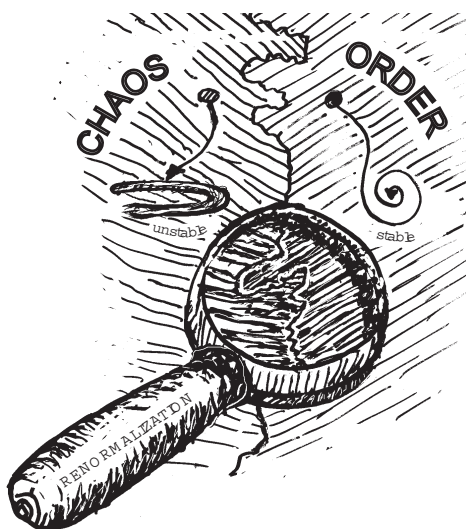


Figure 32.1: Renormalization is the process of magnifying a neighborhood of the border of order, and inspecting closer and closer returns for longer and longer times.

32.1 Holomorphic dynamics

We shall study properties of the asymptotic iterates of

$$z_{n+1} = f(z_n), \quad (32.1)$$

where $f(z)$ is a polynomial in the complex variable z with a quadratic critical point, i.e., with Taylor series expansion of the form

$$f(z) = a_0 + a_2(z - z_c)^2 + \dots$$

Typical model mappings of this type are the Fatou and Julia maps, respectively:

$$f(z) = \lambda - z^2 \quad (32.2)$$

$$f(z) = \lambda z(1 - z). \quad (32.3)$$

When such mappings are used to model dynamical systems with z a real variable and the “nonlinearity” parameter λ real, the asymptotic attractor is conveniently represented by a “bifurcation tree” of figure 31.13, i.e., by a 2-dimensional plot with λ as one axis and values of the asymptotic iterates for given λ plotted along the other axis.

It is not possible to visualize asymptotics of complex iterations in this way, as their iteration space has two (real) dimensions, and period n -tuplings are induced by tuning a pair of (real) parameters. To describe the asymptotic iterates of complex maps we proceed in two steps.

First, we describe the parameter space by its *Mandelbrot set* M . The Mandelbrot set is the set of all values of the mapping parameter (parameter p in the model mapping (32.2)) for which iterates of the critical point do not escape to infinity. A *critical point* z_c is a value of z for which the mapping $f(z)$ has vanishing derivative, $f'(z_c) = 0$. For example $z = 0$ in (32.2) is the critical point. The Mandelbrot set for the mapping (32.2) is plotted in figure 32.2.

Figure 32.2: (a) The Mandelbrot set. Gray: critical point trajectory converges to an attractive periodic orbit of period 1, 2, . . . , 6. White: the critical point trajectory escapes to infinity. Julia sets for the quadratic map $z_{k+1} = \lambda - z^2$ parameter values (b) $\lambda = 0.5$, (c) $\lambda = 0.8$, (d) $\lambda = 1.42$, (e) $\lambda = 0.5 + 0.7i$, (f) $\lambda = 0.123 - 0.745i$, (g) $\lambda = 0.0315 - 0.7908i$, (h) $\lambda = -0.282 + 0.530i$, (i) $\lambda = 1.16 + 0.25i$. (from ref. [3])

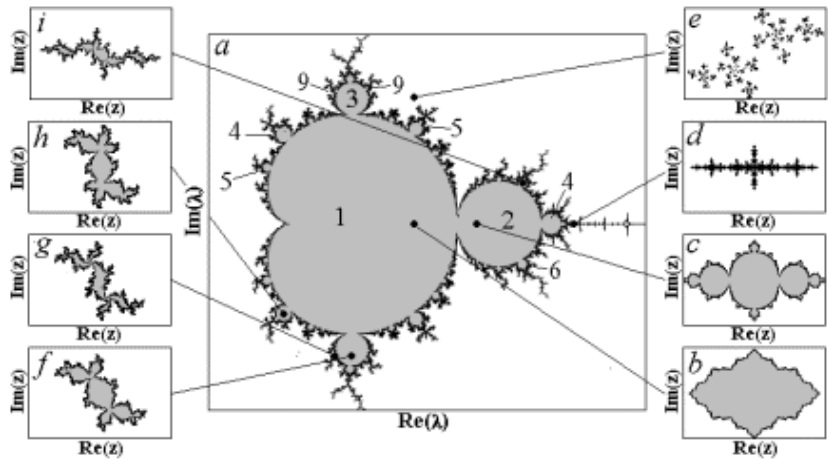
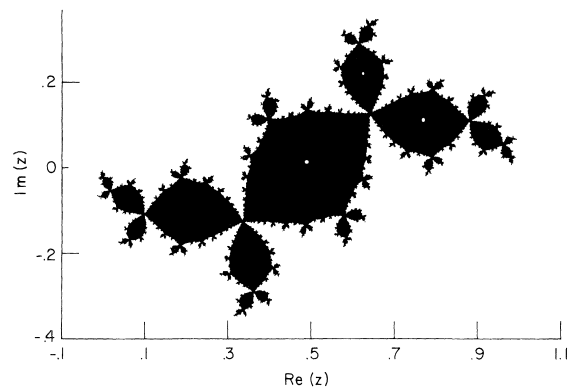


Figure 32.3: The basin of attraction for the superstable 3-cycle of mapping (32.3), $\lambda = 0.123 - 0.745i$. Any initial z from the black region converges toward the superstable 3-cycle, denoted by the three white dots. The basin of attraction for mapping (32.2) superstable 3-cycle is the same, up to a coordinate shift and rescaling.



Second, we characterize the *asymptotic iterates* for a given value of the parameter either by their *basin of attraction*, or by their *attractor*. The basin of attraction K is the set of all values of z which are attracted toward the attractor under iteration by $f(z)$. A typical basin of attraction is plotted in figure 32.3.

The boundary of K , or the *Julia set* J , is the closure of all unstable fixed points of all iterates of $f(z)$.

Theorem. For parameter values within the Mandelbrot set M , the Julia set J is connected. If all critical points iterate to infinity, J is a Cantor set.

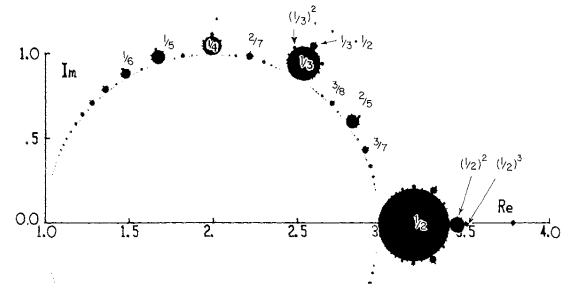
If the n th iterate of $f(z)$ equals z , the set of points $z_k = f^k(z_0)$, $k = 0, 1, 2, \dots, n-1$ form a periodic orbit (or cycle) of length n . If

$$|df^n(z_k)/dz| < 1 \tag{32.4}$$

the cycle is *attractive*, with the *attractor* L the periodic orbit z_0, z_1, \dots, z_{n-1} . If the derivative (32.4) is vanishing, the orbit is *superstable*, and (by the chain rule) a critical point is one of the periodic points. For polynomial mappings $z = \infty$ plays a special role; it is always a superstable fixed point. The following theorem eases attractor searches:

Theorem. The basin of attraction K contains at least one critical point.

Figure 32.4: The Mandelbrot cactus for the Julia mapping (32.3). Inside the big circle (left open for clarity) iterations converge to a fixed point. The full region has two symmetry axes, $\text{Re } \lambda = 1$ and $\text{Im } \lambda = 0$, so only one quarter is shown. The period-doubling sequence is on the real axis. The winding numbers of the periodic orbits corresponding to larger leaves of M are indicated. See ref. [10] for detailed scans of the set.



The precise shape of the Mandelbrot set M depends on $f(z)$, but it always resembles a cactus, see figure 32.4. Here we are not so much interested in the entire M , as in the *Mandelbrot cactus*, the set of components of M generated from a single fixed point by all possible sequences of all possible period n -tuplings.

To summarize, the parameter dependence of asymptotic iterates of mapping $f(z)$ is described by the Mandelbrot set M . For each point inside M , the asymptotic iterates are characterized by their basin of attraction K , the Julia set J and the attractor L .

32.2 Mandelbrot cactus

Now that the general setting is established, we can turn to a detailed study of the way in which a fixed point of the complex mapping (32.1) branches into an n -cycle. The fact that the same analysis applies to period n -tupling of any k -cycle into an nk -cycle will be seen to be the origin of the self-similarity of the Mandelbrot cactus.

Denote the stability of a fixed point by

$$\Lambda = \frac{d}{dz}f(z). \tag{32.5}$$

Example 32.1 Border of fixed-point stability: Fixed point condition for map (32.2), $z^2 + z - \lambda = 0$ yields fixed points. The one of interest here is

with stability (32.5)

$$\Lambda = f'(z^*) = -2z^* = 1 - \sqrt{1 + 4\lambda}$$

The fixed point loses its stability on the marginal stability curve $\Lambda = e^{i\varphi}$. In the complex λ parameter plane, $\varphi = [0, 2\pi]$ traces out a cardioid

$$\lambda = \frac{1}{4}(e^{i2\phi} - ze^{id}), \tag{32.6}$$

the border of the central component of the Mandelbrot set in figure 32.2.

We take, without loss of generality, the fixed point to be at $z = 0$, and $f(z)$ a power series expansion

$$f(z) = \Lambda z + \sum_{j=2}^{\infty} a_j z^j. \quad (32.7)$$

To bring the map into a normal form, we change the variable

$$w = z + \sum_{j=2}^{\infty} h_j z^j, \quad (32.8)$$

and “flatten” out the mapping close to the fixed point by choosing successively h_2, h_3, \dots in such a way that as many leading nonlinear terms as possible vanish in (32.7).

Example 32.2 Smooth conjugacies of a fixed point: *The idea is to perform a smooth nonlinear change of coordinates that flattens out the vicinity of a fixed point and makes the map linear in an open neighborhood. This can be implemented only for an isolated nondegenerate fixed point (as we shall see here, higher terms will contribute to the normal form expansion around the point), and only in a finite neighborhood of a point, as the conjugating function in general has a finite radius of convergence. For example, a quadratic map has two zeros, and there is no global linear map that can capture more one zero.*

Let the fixed point of analytic function $f(z)$ be $z = 0$ and the stability of that point be $\Lambda = f'(0)$. If $|\Lambda| \neq 1$, there exists a smooth conjugation $h(x)$ satisfying $h(0) = 0$ such that:

$$f(z) = h(\Lambda h^{-1}(z)). \quad (32.9)$$

In several dimensions, Λ is replaced by the Jacobian matrix, and one has to check that its eigenvalues are non-resonant, that is, there is no integer linear relation between their logarithms. If $h(z)$ is a conjugation, so is any scaling $h(\alpha z)$ of the function for a case number α . Hence the value of $h'(0)$ is not determined by the functional equation (32.9); we shall set $h'(0) = 1$.

To compute the conjugation h we use the functional equation $h(\Lambda z) = f(h(z))$ and the expansions

$$\begin{aligned} f(z) &= \Lambda z + z^2 f_2 + z^3 f_3 + \dots \\ h(z) &= z + z^2 h_2 + z^3 h_3 + \dots \end{aligned} \quad (32.10)$$

In the present context absorbing the factorials into the definition of expansion coefficients turns out to be more convenient than the usual Taylor expansion. Equating recursively coefficients in expansions in terms of $z=h(u)$

$$\begin{aligned} h(\Lambda u) - \Lambda h(u) &= \sum_{m=2}^{\infty} f_m (h(u))^m \\ \sum_{n=2}^{\infty} (\Lambda^n - \Lambda) h_n u^n &= \sum_{m=2}^{\infty} f_m u^m \left(1 + \sum_{k=2}^{\infty} h_k u^{k-1} \right)^m \end{aligned} \quad (32.11)$$

yields

$$h_2 = \frac{f_2}{\Lambda(\Lambda - 1)}, \quad h_3 = \frac{2f_2^2 + \Lambda(\Lambda - 1)f_3}{\Lambda^2(\Lambda - 1)(\Lambda^2 - 1)}, \quad \dots \quad (32.12)$$

As long as $|\Lambda| \neq 1$, all is well. But if Λ is n -th root of unity $\Lambda = e^{2\pi}$ prefactor in the conjugation (32.11) vanishes, u^n can not be eliminated, justify the local normal for (32.14).

We find it convenient to factorize h_n as

$$h_n = \frac{b_n}{D_n}, \quad D_n = \left(1 - \frac{1}{\Lambda}\right) \left(1 - \frac{1}{\Lambda^2}\right) \cdots \left(1 - \frac{1}{\Lambda^{n-1}}\right) \Lambda^{\frac{(n+2)(n-1)}{2}}.$$

Computer algebra then yields

$$\begin{aligned} b_2 &= f_2 \\ b_3 &= 2f_2^2 + \Lambda(\Lambda - 1)f_3 \\ b_4 &= (5 + \Lambda)f_2^3 - \Lambda(5 - 2\Lambda - 3\Lambda^2)f_2f_3 + \Lambda^2(\Lambda - 1)(\Lambda^2 - 1)f_4. \end{aligned} \tag{32.13}$$

If Λ is sufficiently close to n th root of unity, $\omega = \exp(i2\pi m/n)$, and z is close to 0, the typical behavior of the new iteration function is the same as

$$f(z) = \Lambda z + z^{n+1}. \tag{32.14}$$

The normal function (32.14) has an n -cycle

$$z_j = \omega^j z_0, \quad z_0^n = \omega - \Lambda. \tag{32.15}$$

For $\Lambda = \omega$ this n -cycle coincides with the fixed point $z = 0$. In the neighborhood of $\Lambda = \omega$ we have

$$\begin{aligned} \frac{dz_n}{dz_0} &= f'(z_0)f'(z_1)\cdots f'(z_{n-1}) = \left(\Lambda + (n+1)z_0^n\right)^n \\ &= 1 - (\Lambda - \omega)n^2/\omega + \dots \end{aligned} \tag{32.16}$$

For $\Lambda = (1 + \epsilon)\omega$ the n -cycle (32.15) of the mapping (32.14) is stable if

$$|1 - n^2\epsilon| < 1, \tag{32.17}$$

while the fixed point is stable if

$$|1 + \epsilon| < 1. \tag{32.18}$$

The mapping (32.14) is equivalent to (32.7) only for small z , so the above analysis of how a fixed point of (32.7) becomes unstable and branches into the n -cycle is valid only for infinitesimal $n\epsilon$.

In conclusion, whenever a fixed point becomes unstable at $\Lambda = n$ th root of unity, it branches into an n -cycle which immediately becomes stable. As any stable cycle becomes unstable in the same fashion, branching into a new stable cycle with a multiple of the original cycle length, and as any such cycle is stable inside a disklike region in the complex parameter plane, the union of all these stability regions form a self-similar *Mandelbrot cactus* of figure 32.4.

Next we turn to a study of infinite sequences of period n -tuplings, each branching characterized by the same ratio m/n .

As discussed above, a stable n^k -cycle becomes unstable and branches into an n^{k+1} -cycle when the parameter λ passes through a value such that the stability $\Lambda_k(\lambda)$ (as defined in (32.5)) is the n th root of unity,

$$\Lambda(\lambda) = \omega = e^{i2\pi m/n}.$$

For λ sufficiently close to this value the system is modeled by (32.14). From (32.16) it follows that near the transition from an n^k -cycle to an n^{k+1} -cycle

$$\Lambda_{k+1} = 1 - (\Lambda_k - \omega)n^2/\omega + \dots, \quad (32.19)$$

hence

$$\left. \frac{d\Lambda_{k+1}}{d\lambda} \right|_{\Lambda_{k+1}=1} = -\frac{n^2}{\omega} \left. \frac{d\Lambda_k}{d\lambda} \right|_{\Lambda_k=\omega}, \quad (32.20)$$

and at the transition there is a scale change by the complex factor $-n^2/\omega$ which is independent of k .

32.3 Renormalization and universality

Each leaf of the Mandelbrot cactus figure 32.4 corresponds to an m/n cycle, and the parameter value for the superstable m/n cycle corresponds to the center of the leaf. The above argument suggests that the leaf is approximately n^2 times smaller than the cactus, and that it is rotated by a phase factor $-1/\omega$. The very geometry of the Mandelbrot cactus, figure 32.4, suggests such scaling. This scaling is not exact, because the above analysis applies only to the infinitesimal neighborhood of the junction of a leaf to the cactus; however, the evaluation of the exact scaling numbers shows that this is a rather good approximation to the exact scaling. Numerical evaluation of $\delta_{m/n}$'s supports the conjecture that $\delta_{m/n} \rightarrow -n^2/\omega$ as $m/n \rightarrow 0$, exactly.

The exact scaling is obtained by comparing values of the parameter λ corresponding to successive $(m/n)^k$ superstable cycles, i.e., λ values such that $\Lambda_k(\lambda_k) = 0$. As each cactus leaf is similar to the entire cactus, the ratios of the sizes of the successive stability regions corresponding to successive $(m/n)^k$ -cycles tend to a limit as $k \rightarrow \infty$:

$$\delta_{m/n} = \lim_{k \rightarrow \infty} \frac{\lambda_k - \lambda_{k-1}}{\lambda_{k+1} - \lambda_k}. \quad (32.21)$$

The scaling number δ tells us by how much we have to change the parameter λ in order to cause the next m/n period n -tupling. $\delta_{1/2} = 4.669\dots$ is the Feigenbaum δ for the period doublings in the real 1-dimensional mappings, discussed in chapter 31.

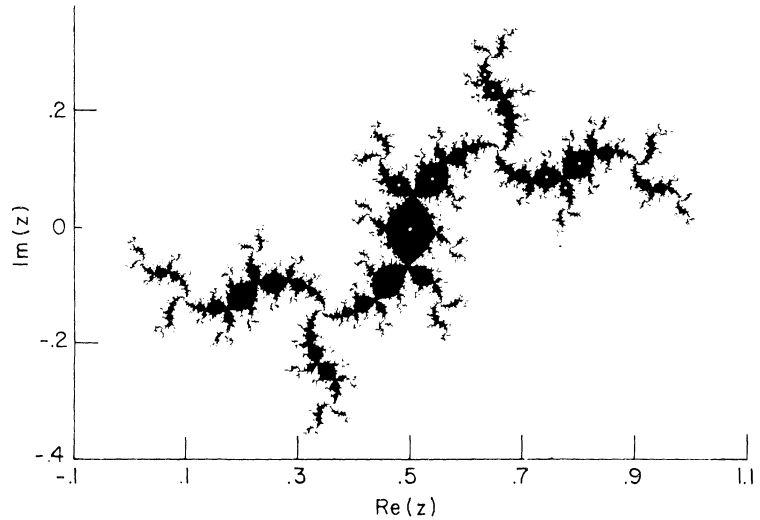


Figure 32.5: The basin of attraction for the superstable 9-cycle for iterates of the model mapping (32.3). The scaled down version of the 3-cycle basin of attraction, figure 32.3, is visible in the center.

Scaling in the parameter space (generalized Feigenbaum δ) is a consequence of the self-similarity of the Mandelbrot cacti. In the same way the self-similarity of the Julia sets (or the asymptotic attractors) suggests a scaling law in the iteration space z , which we discuss next. This law will characterize the scales of successive trajectory splittings (generalized Feigenbaum α).

The self-similarity we are alluding to can be seen by comparing the basin of attraction for the superstable 3-cycle, figure 32.3, and for the superstable 9-cycle, figure 32.5. In the latter figure the 3-cycle basin of attraction is visible in the center, rotated and scaled down by a factor whose asymptotic limit is the generalization of Feigenbaum α to period triplings.

This scaling number α can be computed by comparing the successive superstable cycles, at successive parameter values λ_k, λ_{k+1} . As $k \rightarrow \infty$, the sequence of λ 's converges to λ_∞ , and the superstable n^k -cycles converge to an n^∞ -cycle. The attractor is self-similar: the orbits on succeeding levels are related by rescaling and rotation by a complex number which asymptotically approaches

exercise 32.1

$$\alpha_{m/n} = \lim_{k \rightarrow \infty} \frac{z_{n^k} - z_0}{z_{n^{k+1}} - z_0}. \tag{32.22}$$

α characterizes the scale of trajectory splitting at each period n -tupling. For $m/n = 1/2$ this is the Feigenbaum $\alpha = -2.5029\dots$,

So period n -tuplings are self-similar both in the iteration space and in the parameter space: not only does the asymptotic orbit resembles itself under rescaling and rotation by α , but also each leaf of the Mandelbrot cactus resembles the entire cactus under rescaling and rotation by δ .

These self-similarities can be described by means of the following three operations:

The first operation is a rescaling of the parameter and iteration spaces:

$$[Rf]_p(z) = af_{p/d}(z/a). \tag{32.23}$$

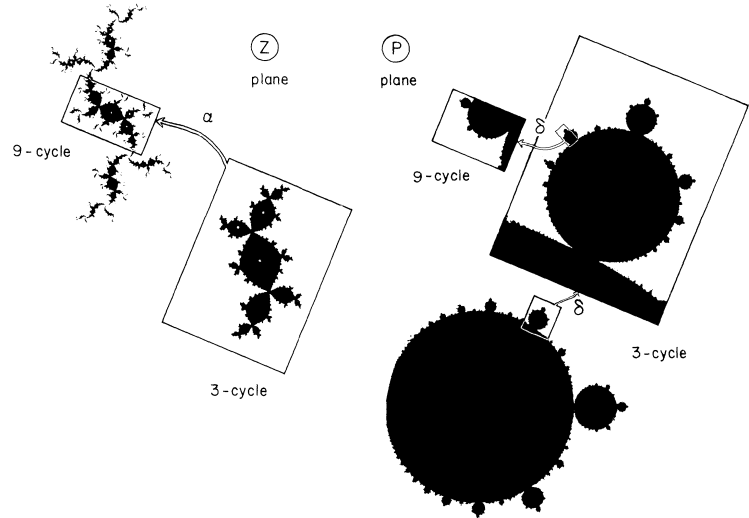


Figure 32.6: The unstable manifold method illustrated by period triplings. The parameter is shifted from the center of a cactus leaf to its 1/3 leaf, the 1/3 leaf is rescaled and rotated by δ , and the basin of attraction of third iterates is rescaled and rotated by α . The Mandelbrot cactus and the basin of attraction for the unstable manifold $g_p(z)$ is self-similar under such shifting and rescaling.

With the appropriate choice of complex numbers d and a , a leaf of the Mandelbrot cactus (a part of the attractor) can be rescaled and rotated to approximately overlap the entire cactus (entire attractor, respectively).

We fix the origin of p and z by requiring that $z = 0$ be a critical point of the mapping $f_p(z)$, and, for the parameter value $p = 0$, a superstable fixed point as well. Mapping (32.2) is an example. We fix the scale of p and z by requiring that the superstable m/n cycle occurs for the parameter value $p = 1$ and that

$$f_1(0) = 1. \tag{32.24}$$

The second operation shifts the origin of the parameter space to the center of the m/n -leaf of the Mandelbrot cactus (p corresponding to the superstable m/n cycle):

$$[Sf]_p(z) = f_{1+p}(z). \tag{32.25}$$

The third operation iterates $f_p(z)$ n times:

$$[Nf]_p(z) = f_p^n(z). \tag{32.26}$$

By definition, $[Sf]_0(z) = f_1(z)$ has a superstable m/n cycle, so its n th iterate has a superstable fixed point, $[NSf]_0(0) = 0$.

The parameter shift S overlays the Mandelbrot cactus over its m/n leaf, and the Julia set for $[Nf]_1(z)$ resembles the Julia set for the superstable fixed point $f_0(z)$ (compare figure 32.3 with figure 32.5, for example). Finally we adjust the scale of the new M, J sets by requiring that the scale factors a, d in (32.23) are such that $[RNSf]_p(z)$ satisfies the same normalization condition (32.24) as the initial function $f_0(z)$. This shifting and rescaling is illustrated in figure 32.6.

The combined effect of the rescaling, parameter shift and iteration is summarized by the operator $T^* = RNS$

$$[T^*f]_p(z) = af_{1+p/d}^n(z/a). \tag{32.27}$$

If we take a polynomial $f_p(z)$ and act on it with T^* , the result will be a longer polynomial with similar M and J sets. For a finite number of T^* operations the scaling numbers d and a depend on the choice of the initial mapping $f_p(z)$. If we apply T^* infinitely many times, a and d converge to the universal numbers α and δ , and $T^* f_p(z)$ converges to a one-parameter family of universal functions which is the fixed line of the operator T^* :

$$g_p(z) = [T^* g]_p(z) = \alpha g_{1+p/\delta}^n(z/\alpha). \quad (32.28)$$

This universal equation determines both $g_p(z)$ and the universal numbers α and δ . The 1-dimensional family of universal functions $g_p(z)$ parameterized by p is called the *unstable manifold*.

To summarize, the T^* operation encodes simultaneously the self-similarity of the parameter space (Mandelbrot cacti) and of the iteration space (Julia sets). Being no more than a redefinition of variables, it is an explicit implementation of the above self-similarities; T^* magnifies the n th iterate of the $(m/n)^{k+1}$ -cycle and overlays it onto the $(m/n)^k$ -cycle (see figure 32.6). Asymptotically the self-similarities are exact, and the procedure converges to the unstable manifold, a 1-dimensional line of universal functions g_p .

Not only are the N , S , R operations the natural encoding of the complex universality, but they also turn out to be powerful computational tools.

The universal equation (32.28) can be solved numerically by approximating the unstable manifold by a truncation of the double power series expansion

$$g_p(z) = \sum_{j,k \geq 0}^{N,M} c_{jk} z^{2j} p^k. \quad (32.29)$$

We start with (32.2) as a two term approximation to $g_p(z)$. Repeated applications of the T^* operation (32.27) generate a longer and longer double polynomial in z and p ; this procedure converges asymptotically to the unstable manifold $g_p(z)$. We implement the shifting and iteration operations S and N as numerical polynomial substitution routines, truncating all polynomials as in (32.29). The T^* operation is completed by the rescaling operation R , equation (32.23). The scaling numbers d and a are fixed by the normalization conditions (32.24). We use the Newton method to find the parameter value corresponding to the superstable m/n -cycle. This determines d , and a then follows directly from the condition (32.24). The result is a new approximation to $g_p(z)$. Asymptotically d 's converge to δ and a 's converge to α . We keep applying the truncated T^* operation until the coefficients in (32.29) stabilize to desired accuracy.

The self-similar structure of the Mandelbrot cactus, figure 32.4, suggests a systematic way of presenting the universal numbers that we have computed in the previous section. Observe that roughly halfway between any two large leafs on the periphery of a Mandelbrot cactus (such as $1/2$ and $1/3$) there is the next largest leaf (such as $2/5$). Furthermore, we know from (32.20) that the size of the ‘‘cactus leaf’’ corresponding to period n -tupling is of order n^{-2} . Hence the natural hierarchy is provided by an interpolation scheme which organizes rational

numbers m/n into self-similar levels of increasing period lengths n . Such scheme is provided by Farey numbers.

Implicit in the Farey numbers are scaling laws that relate the universal numbers. It turns out that the same Farey structure is a very useful tool for the study of mode-locking intervals for circle maps. We shall discuss this at length in chapter 33.

Exercises

32.1. Approximate period tripling renormalization:

Implement an approximate renormalization for period-tripling sequence of figure 32.6, using the approximate period-doubling renormalization scheme of example 31.3, applied to the complex polynomial

$$z_{n+1} = \lambda - z_n^2.$$

The idea is to drop from $f_\lambda \circ f_\lambda \circ f_\lambda(z)$ all terms higher than z^2 in each period-tripling step. Evaluate numerically the complex coordinate and parameter rescaling universal constants $\alpha_{1/3}$ and $\delta_{1/3}$.

(O.B. Isaeva and S.P. Kuznetsov)

References

- [32.1] B.B. Mandelbrot, “Fractal aspects of the iteration $z \rightarrow \lambda z(1-z)$ for complex λ and z ,” *Nonlinear Dynamics*, ed. R.H.G. Helleman, *Annals of New York Academy of Sciences* **357**, 249 (1980);
- [32.2] B.B. Mandelbrot, *The Fractal Geometry of Nature* (Freeman, San Francisco, 1983).
- [32.3] O.B. Isaeva and S.P. Kuznetsov, “On possibility of realization of the phenomena of complex analytic dynamics in physical systems. Novel mechanism of the synchronization loss in coupled period-doubling systems,” [arXiv:nlin.CD/0509012](https://arxiv.org/abs/nlin.CD/0509012).
- [32.4] O.B. Isaeva and S.P. Kuznetsov, “On possibility of realization of the Mandelbrot set in coupled continuous systems,” [arXiv:nlin.CD/0509013](https://arxiv.org/abs/nlin.CD/0509013).
- [32.5] O.B. Isaeva and S.P. Kuznetsov, “Period-tripling accumulation point for complexified Hénon map,” [arXiv:nlin.CD/0509015](https://arxiv.org/abs/nlin.CD/0509015).
- [32.6] P. Cvitanović and J. Myrheim, “Universality for period n -tuplings in complex mappings,” *Phys. Lett.* **A94**, 329 (1983);
- [32.7] “Complex universality,” *Commun. Math. Phys.* **121**, 225 (1989).

- [32.8] P. Cvitanović, “Renormalization description of transitions to chaos,” in S. Lundquist, N.H. March and E. Tosatti, eds., pp. 73-97, *Order and Chaos in Non-linear Physical Systems* (Plenum, New York 1988).
- [32.9] A.I. Golberg, Y.G. Sinai and K.M. Khanin, “Universal properties for sequences of bifurcations of period 3,” *Usp. Mat. Nauk* **38**, 159 (1983).
- [32.10] E. Demidov, “Anatomy of Mandelbrot and Julia sets,”
www.ibiblio.org/e-notes